

Failure mechanism of polyamide 66 nanofiber yarns under fatigue and static tensile loading

Sara Asghari Mooneghi,¹ Ali Akbar Gharehaghaji,¹ Hossein Hosseini-Toudeshky,² Giti Torkaman³

¹Department of Textile Engineering, Amirkabir University of Technology, Tehran, Iran

²Department of Aerospace Engineering, Amirkabir University of Technology, Tehran, Iran

³Department of Physical Therapy, Tarbiat Modares University, Tehran, Iran

Correspondence to: A. A. Gharehaghaji (E-mail: aghaji@aut.ac.ir)

ABSTRACT: This work aims at fractography of polyamide 66 nanofiber yarns. The yarns are produced with three twist levels via electrospinning. In order to study the fracture modes of nanofiber yarns, fatigue, and static tensile tests including monotonic, low cycle fatigue, and postcyclic monotonic tensile tests are performed. It is observed that the catastrophic failure of yarns is associated with axial splitting in the three categories. The nanofibers within the yarn structure show a ductile fracture and buckle after tensile stress release. In comparison of postcyclic monotonic tensile tests with other categories, nanofibers show severe plastic buckling in response to release of the same applied force. Fractography studies reveal that twisting causes construction of a layered structure in the yarns which is similar to the ideal yarn structure as well. Applying cyclic loading causes the separation of these structural layers which is more considerable under higher number of cycles. © 2015 Wiley Periodicals, Inc. *J. Appl. Polym. Sci.* **2015**, *132*, 41925.

KEYWORDS: electrospinning; fatigue; fractography; nanofiber yarn; tensile properties

Received 12 August 2014; accepted 2 January 2015

DOI: 10.1002/app.41925

INTRODUCTION

Electrospun nanofibers have splendid properties, such as super-fine scale, large specific surface area, and porosity. Thus, they have a high potential to be used in applications, such as tissue engineering, biomaterials, textiles, electronics, photonics, aerospace, and industrial filtration. However, nanofibers cannot be used in a single form due to the low strength and handling problems. Generally, electrospun fibers are collected in the form of nonwoven mats which have limited applications due to their relatively low mechanical strength.^{1–3} Recently, electrospun nanofiber yarns with load bearing capability have attracted considerable attention. Several studies were reported towards developing these yarns in which special attention was mainly paid to their tensile static properties.^{1,4–10}

Some researches were performed on the fracture modes of single nanofibers after monotonic tensile tests. Zussman *et al.*¹¹ showed that poly(ethylene oxide) nanofibers failed by a multiple necking mechanism which was sometimes followed by the development of a fibrillar structure. A two-stage rupture behavior of the nanotube–polyacrylonitrile composite nanofibers under tension including crazing of the polymer matrix and pullout of carbon nanotubes, was observed by Ye *et al.*¹² Naraghi *et al.*¹³ studied the mechanical deformation and failure of electrospun polyacrylonitrile nanofibers as a function of strain

rate. Gharehaghaji and Denning¹⁴ studied the fracture modes of various nanofibers such as polystyrene and polyamide (PA) under tensile stresses. In their study, an array of nanofibers was ruptured in a ductile form. It was found that the porosity of nanofibers had a governing effect in the fracture behavior. Buckling of nanofibers was also clearly observed after releasing from extension.

In the field of nanofibrous yarn fracture, Sui *et al.*⁹ studied the fracture of electrospun polymethyl methacrylate yarns after static tensile tests. Researchers found that the minute addition of sodium chloride (NaCl) in the solution during electrospinning not only significantly enhanced the mechanical properties of nanofibers, but also changed the failure ends of yarns under tensile forces due to different fiber–fiber interactions. The pristine yarn remained integrated during failure, reflecting strong fiber–fiber interactions while the nanofibers in the failure end of the NaCl-mediated yarn were almost completely disconnected from each other, reflecting poor fiber–fiber interactions.

To the authors' knowledge, little is known regarding the tensile fatigue properties of nanofibrous yarns and their corresponding fracture modes. In our previous work,¹⁵ we studied the tensile fatigue behavior of continuous PA66 nanofiber yarns. The results showed that applying fatigue loading caused an increase in the alignment of nanofibers within the yarn structure and

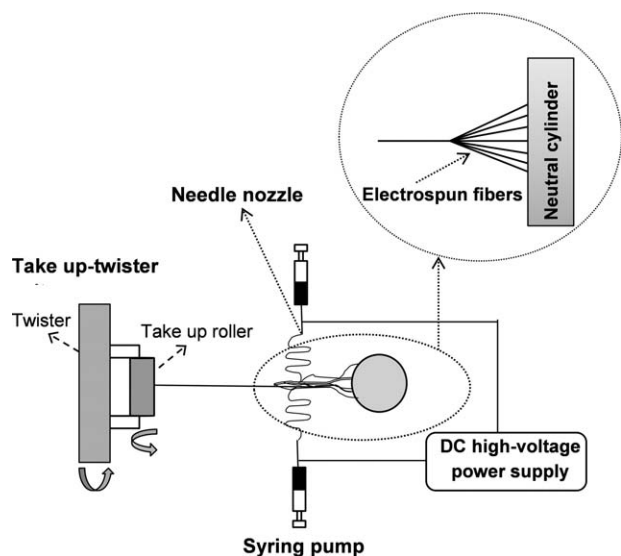


Figure 1. The experimental setup for electrospinning of nanofiber yarns.

crystallinity which could be interpreted as improved ultimate stress and elastic modulus. In the present work, continuous PA66 nanofiber yarns were fabricated with three different twist levels via the electrospinning method using two oppositely charged nozzles. Fatigue and static tensile tests were performed to examine the fracture modes for three loading categories: monotonic, low cycle fatigue and postcyclic monotonic tensile loadings.

EXPERIMENTAL

Materials

A suitable polymer solution was prepared for electrospinning by dissolving 16 wt % pure PA66 (Sigma-Aldrich) in formic acid (Merck). In order to have homogeneity, the polymer solution was stirred for 5 h at the ambient condition.

Figure 1 illustrates the experimental setup used to produce electrospun nanofiber yarns. The setup consists of two needle nozzles, a high-voltage DC power supply (max 25 kV), two syringe pumps (TOP-5300), a neutral cylinder (6 cm diameter \times 30 cm length), a twister with adjustable rotational speed (ranging from 1 to 440 rpm) and a take-up roller controlled by a stepper motor.¹⁵

The electrospinning was carried out between the nozzles and the neutral cylinder at room conditions. The applied voltage was 18.5 kV. Since nanofibers were produced with opposite charges from the nozzles, they attracted each other and their surface charges declined to zero on the neutral surface. During electrospinning, the take-up twister unit was located between the nozzles at the distance of 240 mm. Two oppositely charged nozzles were placed on both sides of the neutral cylinder at the distance of 25 mm. The distance between two nozzles was set at 180 mm. A piecing yarn was attached to the take-up roller and its tail met the convergence point of electrospun fibers. Electrospun fibers were twisted by rotating the piecing yarn around its axis via the twister immediately after getting in contact with the

piecing yarn tail. The electrospun nanofiber yarn was wound on the take-up roller with a constant speed. In this case, the other end of the nanofibers on the surface of the neutral cylinder was drafted towards the take up-twister unit continuously.¹⁵ The yarns had three different twist levels, i.e., 160, 224, and 288 rpm achieved by changing the rotational speed of the twister. The speed of the take-up roller was remained constant during all of the experiments. Other researchers also used successfully a similar setup.^{6,15}

Morphology and Fracture Study

Morphology, mechanical deformation, and fracture modes of the specimens were observed under a scanning electron microscope (SEM, Philips XL30). The fracture modes of the specimens were studied after monotonic, low cycle fatigue, and postcyclic monotonic tensile loadings.

Differential Scanning Calorimetry

Differential scanning calorimetry (DSC) was used to study the crystallinity of the nanofiber yarns. The heating rate was $10^{\circ}\text{C min}^{-1}$. The yarns were heated up from room temperature to 250°C . The crystallinity (χ_c) was calculated from eq (1):

$$\chi_c (\%) = \frac{\Delta H_m}{\Delta H_m^0} \times 100\% \quad (1)$$

where ΔH_m and ΔH_m^0 show the melting enthalpy and the melting enthalpy of 100% crystalline PA66 (255.8 J g^{-1}),¹⁶ respectively.

Mechanical Tests

The Zwick/Roell Z2.5 tensile tester was used to measure the tensile properties of nanofiber yarns at room condition. The gauge length was 100 mm. The number of tests was 30 for monotonic tensile tests. The crosshead speed of 50 mm/min was chosen for the monotonic and postcyclic monotonic tensile tests.

The load controlled tensile fatigue tests were performed with crosshead speed of 300 mm/min and R ratio of 0.8 on three specimens in each test group. The loading amplitude was 78 and 82% of the yarn average ultimate load for each twist level. All of the nanofiber yarns were tested for the number of cycles required to reach the catastrophic failure for determining the life cycle. Due to device limitations, the maximum number of 2000 cycles was applied to the specimens. The specimens that had not ruptured by 2000 cycles were totally unloaded at the end of the 2000 cycles. Then after 5 min, they were again subjected to a monotonic tensile test to study their modes of fracture. Only in case of loading amplitude of 78%, the specimens did not rupture after 2000 cycling.

RESULTS AND DISCUSSION

SEM images of nanofiber yarns with various twist levels, i.e., 160, 224, and 288 rpm showed that the mean diameter of yarns was 222, 209, and 133 μm and the mean diameter of nanofibers was 259, 253, and 252 nm, respectively. Table I shows the average values of life cycle, crystallinity (χ_c), ultimate stress, ultimate strain, and elastic modulus for three test groups. All of the mentioned parameters (except life cycle) were measured for monotonic and postcyclic monotonic tensile tests.

Table I. The Results from DSC and Tensile Tests

Test group		1	2	3
Twist rate (rpm)		160	224	288
Life cycle	78%	(2000)	(2000)	(2000)
	82%	669	796	686
χ_c (%)	a	23	12	17
	b	27	20	26
Average ultimate stress (MPa)	a	64	64.2	88.4
	b	82.5	82.1	116.1
Average ultimate strain (%)	a	40.6	41.4	40
	b	12.5	18.7	17.5
Average elastic modulus (MPa)	a	213.2	216.5	363.1
	b	612.1	540.2	745.5

^a The average values from monotonic tensile tests.

^b The average values from postcyclic monotonic tensile tests.

Fracture Study: Monotonic Tensile Test

Figure 2 illustrates the typical failure mechanism of the nanofiber yarns after monotonic tensile tests. The nanofibers within the yarn structure [Figure 2(C,F)] presented a ductile failure due to the necking prior to rupture. The necking mechanism before final failure was reported for the various nanofibers such as PA already.^{11–14} Buckling of nanofibers also seemed to be a common phenomenon after releasing from extension [Figure 2(C,E)] which was in good agreement with the reported observations in a previous work.¹⁴

Axial splitting was the dominant type of deformation of nanofiber configuration in the yarns which was hindered in the nanofiber yarns with higher twist levels. The length of the oblique fracture surface [Figure 2(A,D)] was typically dependent to the twist level. In a twisted nanofibrous yarn, radial forces were developed within the inter-structure of yarn due to twist-

ing. This resulted in further cohesion of the nanofibers. In a twisted yarn, rupture of fibers occurs one by one which gradually leads to the catastrophic failure. This could be hindered by the amount of twist level. As indicated in Table I, there was an increase in the average values of both ultimate stress and elastic modulus during monotonic tensile tests when the twist rate changed from 160 to 288 rpm. Higher twist leads to larger radial forces which cause increasing of contact area between the adjacent fibers and result in the fibers to come closer. Hence, the air volume is reduced. This will end up to a reduction in the yarn diameter. Also, we observed a reduction in the diameter of nanofibers due to further extension during insertion of higher levels of twisting. By increasing the twist level from 160 to 288 rpm, the mean diameter of yarns decreased from 222 to 133 μm and the mean diameter of nanofibers decreased from 259 to 252 nm, respectively. Lateral interfaces which keep the

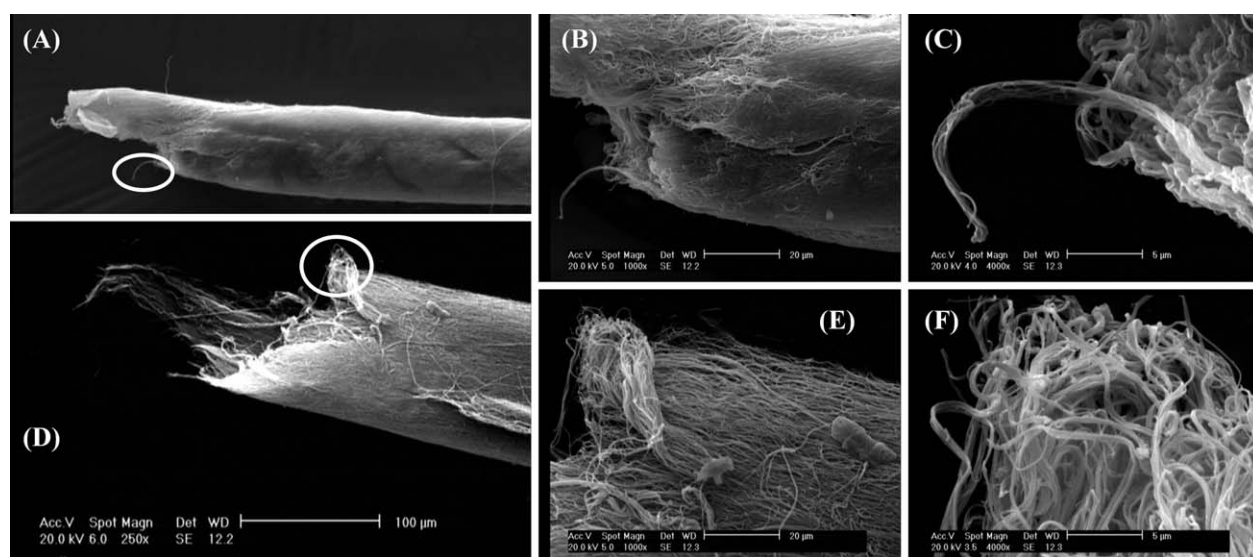


Figure 2. SEM images of a fractured nanofiber yarn with twist rate of 224 rpm after a monotonic tensile test in different magnifications: (A–C) left end in 250 \times , 1000 \times , and 4000 \times magnification, respectively (D–F) right end in 250 \times , 1000 \times , and 4000 \times magnification, respectively.

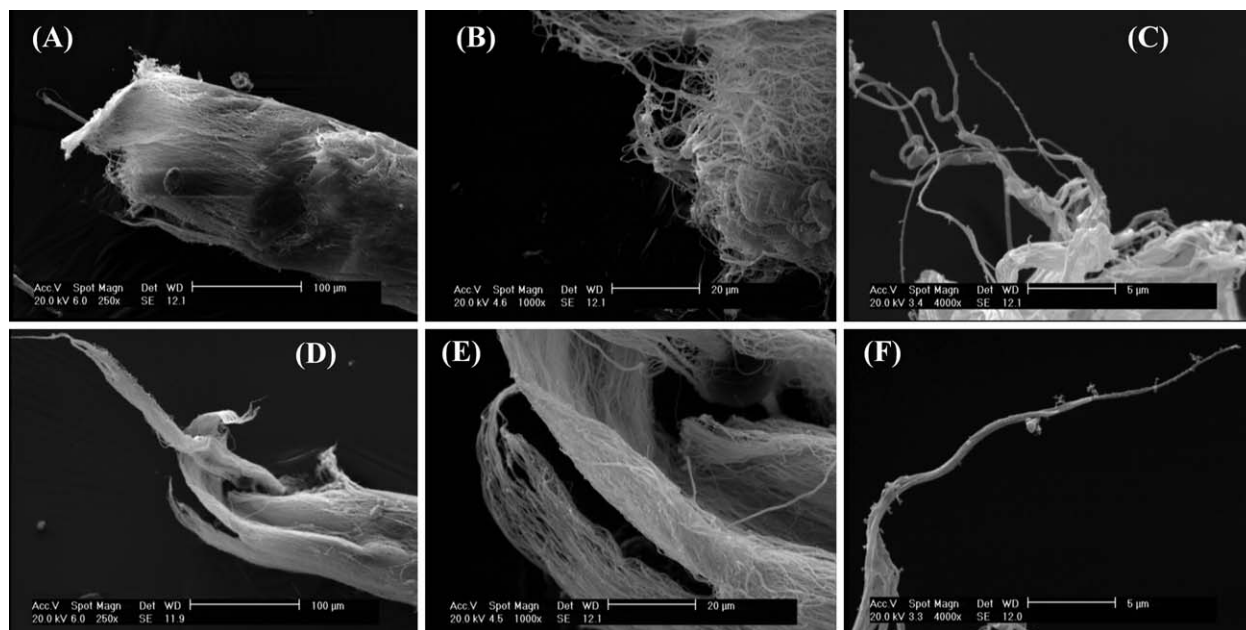


Figure 3. SEM images of a fractured nanofiber yarn with twist rate of 160 rpm after a low cycle fatigue tensile test in different magnifications: (A–C) left end in 250 \times , 1000 \times , and 4000 \times magnification, respectively (D–G) right end in 250 \times , 1000 \times , and 4000 \times magnification, respectively. Loading amplitude was 82% of the yarn average failure load.

nanofibers together in the yarn increased due to larger contact area and caused enhancement in the tensile characteristics. The results were in a very good agreement with the previous reported works.^{1,5–9,15}

Both fractured ends [Figure 2(A,D)] demonstrated strong fiber–fiber interactions within the yarn. Following the catastrophic failure after monotonic tensile loading which was associated with the slippage of adjacent nanofibers, the yarn remained integrated to somehow and nanofibers were not completely disconnected.

Fracture Study: Low Cycle Fatigue Tensile Test

Figure 3 shows the typical failure mechanism of nanofiber yarns subjected to a tensile fatigue test with loading amplitude of 82% of the yarn average failure load. The nanofibers showed a ductile failure behavior due to the necking phenomenon prior to rupture [Figure 3(C,F)]. Buckling of nanofibers was observed after tensile fatigue tests [Figure 3(B,D)]. This phenomenon which was in agreement with the results presented in a previous study,¹⁴ was observed after monotonic tensile tests as well.

It was observed that the fracture of yarns was associated with axial splitting which run around the yarn and then tore along the yarn. Rupture of one nanofiber may cause a region of stress concentration from which axial shear stresses form and propagate to cause the catastrophic failure [Figure 3(A,D)]. By rupturing of more nanofibers in further stretching and loading cycles, this region becomes wider and deeper. Finally, the tensile stresses on the reduced cross section are large enough to cause the catastrophic failure. Several independent regions were formed along the yarn, one of which definitely caused the yarn rupture. Some variants in the fractured ends were also observed after the nanofibers experienced the tensile fatigue. These could be attributed to the shear stresses due to the twisting which

caused stress concentration regions to run in different directions. A similar behavior was seen before for the tensile fatigue of conventional PA66 fibers.¹⁷ Since there are numerous nanofibers within the yarn structure, the failure mechanisms were more complicated in comparison to conventional yarns.

Fracture Study: Postcyclic Monotonic Tensile Test

The failure mechanism of a nanofiber yarn is shown in Figure 4 during a postcyclic monotonic tensile test. The nanofibers exhibited ductile failures [Figure 4(B,C)]. It appeared that in postcyclic monotonic tensile tests, axial splitting was also the dominant mode of deformation. Several independent regions of stress concentration expanded at small angles to the yarn axis which ran in different directions later on.

The buckling [Figure 4(C,E,F)] was severe in comparison to the fatigue and monotonic tensile tests in the case of postcyclic monotonic tensile tests. As shown in Table I, fatigue caused an increase in the crystallinity of the electrospun nanofiber yarns. Crystallinity increases strength and elastic modulus as the secondary bonding is enhanced when the molecular chains are closely packed and parallel. It is also associated with some decrease in elongation.^{15,18,19} Moreover, an increase in crystallinity results in a larger localization of deformation. This phenomenon was shown before for semicrystalline polymers such as PA66.^{18,20} Indeed, applying large number of cyclic loadings resulted in extensive plastic deformation which in return caused the nanofiber yarns to become longer in length and smaller in diameter. Taking into consideration all of the mentioned changes in the structural features and mechanical characteristics of the specimens, the nanofiber yarns experienced large number of tensile cyclic loadings exhibited smaller value of EI (elastic modulus \times area moment of inertia) in comparison to

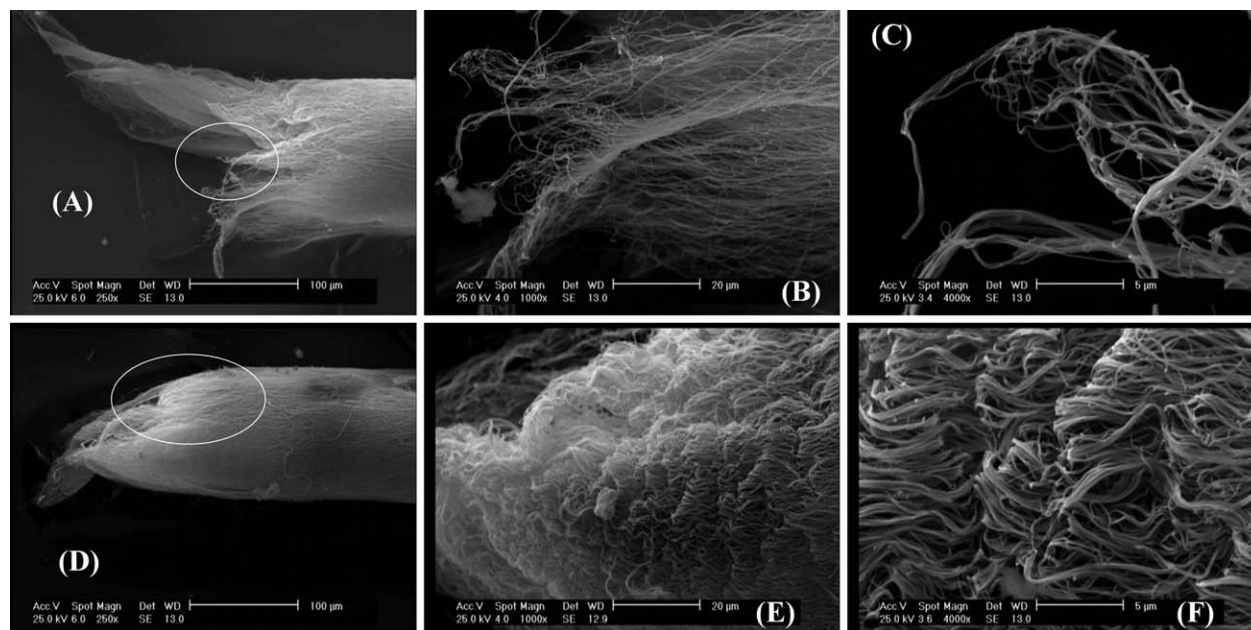


Figure 4. SEM images of a fractured nanofiber yarn with twist rate of 288 rpm after a postcyclic monotonic tensile test in different magnifications: (A–C) left end in 250 \times , 1000 \times , and 4000 \times magnification, respectively (D–F) right end in 250 \times , 1000 \times , and 4000 \times magnification, respectively.

specimens without cyclic loading or low number of cycles. As a result, they showed severe plastic buckled nanofibers in response to releasing from the same applied force.

Investigations on the failure zones of nanofibrous yarns also revealed that twisting caused construction of a layered structure

in electrospun nanofiber yarns which resembled the same structure as the ideal yarn (Figure 5). An idealized twisted yarn structure is assumed to be in a cylindrical form with specific radius. Twisting creates a layered structure in the ideal yarn which comprises of a series of concentric cylinders of differing radii.^{21,22} Comparing the failure ends in all of the three

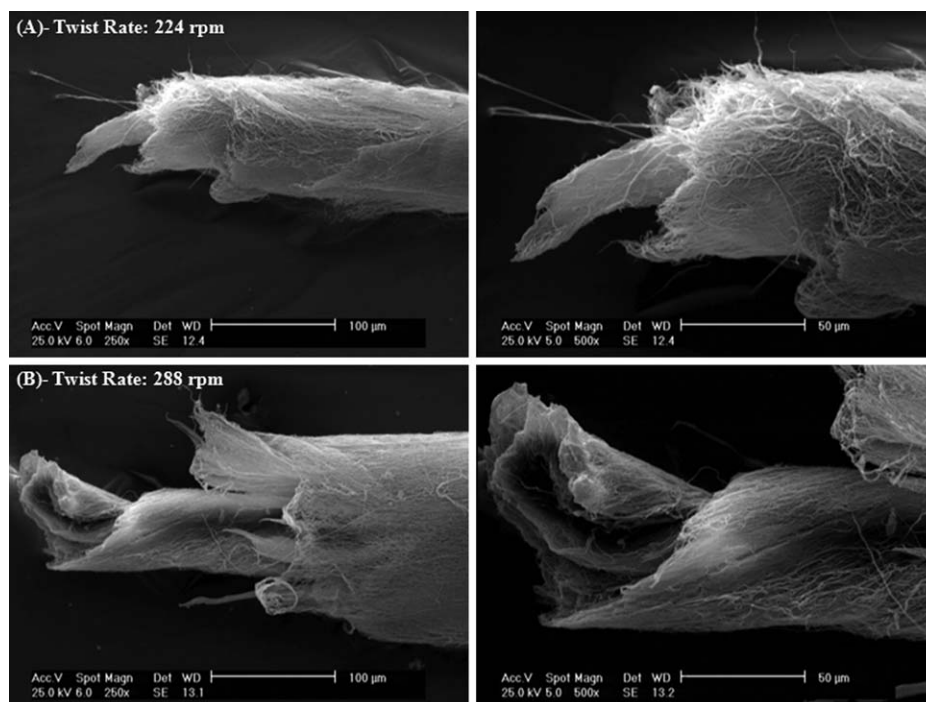


Figure 5. SEM images of PA66 nanofiber yarns with different twist rates which resembled the same structure as an ideal yarn (left: final failure of a yarn, right: final failure of a yarn with a higher magnification): (A) 224 rpm and (B) 288 rpm.

categories also revealed that applying cyclic loading caused the separation of these structural layers. The separation was more pronounced by increasing the number of cycles.

CONCLUSION

This study aimed at investigating the fracture modes in monotonic, low cycle fatigue, and postcyclic monotonic tensile tests of continuous PA66 nanofiber yarns with three different twist rates. Nanofiber yarn failure was found to be associated with axial splitting. The general modes of failure did not show any dependency of fracture to the twist rate. Increasing the twist level created more cohesion between nanofibers which in turn caused hindered axial splitting in case of monotonic tensile tests. Ductile failure and necking prior to rupture were the common feature of the fracture in three various categories of tests. Also, buckling of nanofibers was a common phenomenon after releasing from tension. In tests with high number of cycles, buckling was severe. Moreover, investigations on the failure zones of yarns revealed that twisting created a layered structure in the electrospun yarns, a feature that is seen in the ideal yarn structure. Applying fatigue loading caused the separation of these structural layers which was more notable in application of higher number of cycles.

REFERENCES

1. He, J.; Qi, K.; Zhou, Y.; Cui, S. *J. Appl. Polym. Sci.* **2014**, *131*, 40137.
2. Li, M.; Xiao, R.; Sun, G. *J. Appl. Polym. Sci.* **2012**, *124*, 28.
3. Ramakrishna, S.; Fujihara, K.; Teo, W. E.; Lim, T. C.; Ma, Z. In *An Introduction to Electrospinning and Nanofibers*; World Scientific Publishing: Singapore, **2005**.
4. Chawla, S.; Naraghi, M.; Davoudi, A. *Nanotechnology* **2013**, *25*, 255708.
5. Fennessey, S. F.; Farris, R. *Polymer* **2004**, *45*, 4217.
6. F. Hajiani, F.; Jeddi, A. A. A.; Gharehaghaji, A. A. *Fiber Polym.* **2012**, *13*, 244.
7. Ali, U.; Zhou, Y.; Wang, X.; Lin, T. *J. Textile Indus.* **2012**, *103*, 80.
8. Li, J.; Tian, L.; Pan, N.; Pan, Z. *J. Polym. Eng. Sci.* **2014**, *54*, 1618.
9. Sui, X.; Wiesel, E.; Wagner, H. D. *Polymer* **2012**, *53*, 5037.
10. Yan, H.; Liu, L.; Zhang, Z. *Mater. Lett.* **2011**, *65*, 2419.
11. Zussman, E.; Rittel, D.; Yarin, A. L. *Appl. Phys. Lett.* **2003**, *82*, 3958.
12. Ye, H.; Lam, H.; Titchenal, N.; Gogotsi, Y.; Ko, F. *Appl. Phys. Lett.* **2004**, *85*, 1775.
13. Naraghi, M.; Chasiotis, I.; Kahn, H.; Wen, Y.; Dzenis, Y. *Appl. Phys. Lett.* **2007**, *91*, 151901.
14. Gharehaghaji, A. A.; Denning, R. Fracture of Nanofibers and Environmental Aspects. In *7th International Conference—TEXSCI*, Liberec, Czech Republic, September 6–8; **2010**.
15. Asghari Mooneghi, S.; Gharehaghaji, A. A.; Hosseini-Toudeshky, H.; Torkaman, G. *Polym. Eng. Sci.* **2014**, DOI: 10.1002/pen.24019.
16. Sichina, W. J. DSC as Problem Solving Tool: Measurement of Percent Crystallinity of Thermoplastics; PETech-40; PerkinElmer Instruments, **2000**.
17. Hearle, J. W. S.; Lomas, B.; Cooke, W. D. In *Atlas of Fibre Fracture and Damage to Textiles*, 2nd ed.; Woodhead Publishing: Cambridge, **1998**.
18. Hegde, R. R.; Dahiya, A.; Kamath, M. G.; Kannadaguli, M.; Kotra, R. Nylon Fibers, <http://www.engr.utk.edu/mse/Textiles/Nylon%20fibers.htm>, **2004**. Accessed: 13 Jan, 2015.
19. Chapter 16. Polymers. Characteristics, Applications and Processing, <http://www.virginia.edu/bohr/mse209/chapter16.htm>. Accessed: 13 Jan, 2015.
20. Janssen, R.; Meijer, H. E. H.; Govaert, L. E.; Schellekens, R.; Schrauwen, B. A. G. Deformation and Failure in Semi-Crystalline Polymer Systems, Master Thesis, Eindhoven University of Technology, MT 02.14, **2002**.
21. Mogahzy, Y. E. In *Engineering Textiles: Integrating the Design and Manufacture of Textile Products*, Woodhead Publishing: Cambridge, **2008**; Chapter 9.
22. Hearle, J. W. S.; Grosberg, P.; Backer, S. In *Structural Mechanics of Fibers, Yarns, and Fabrics*, Wiley: New York, **1969**; Vol. 1.